

Short communication

Fluorescence spectroscopic study of serum albumin–bromadiolone interaction: fluorimetric determination of bromadiolone

Subbiah Deepa, Ashok K. Mishra *

Department of Chemistry, Indian Institute of Technology Madras, Chennai 600 036, India

Received 5 August 2004; received in revised form 23 January 2005; accepted 26 January 2005

Available online 24 February 2005

Abstract

Bromadiolone (BRD), a substituted 4-hydroxycoumarin derivative, is known to possess anti-coagulant activity with acute toxicity. In this paper, we report a study on the interaction of bromadiolone with the plasma proteins bovine serum albumin (BSA) and human serum albumin (HSA), using the intrinsic fluorescence emission properties of bromadiolone. Bromadiolone is weakly fluorescent in aqueous buffer medium, with an emission at 397 nm. Binding of bromadiolone with serum albumins (SA) leads to a marked enhancement in the fluorescence emission intensity and steady state fluorescence anisotropy (r_{ss}), accompanied by a blueshift of 10 nm. In the serum albumin–bromadiolone complex, selective excitation of tryptophan (Trp) residue results in emission from bromadiolone, thereby indicating a Förster type energy transfer from Trp to BRD. This quenching of Trp fluorescence by BRD was used to estimate the binding constant of the SA–BRD complex. The binding constants for BRD with BSA and HSA were 7.5×10^4 and 3.7×10^5 L mol⁻¹, respectively. Based on this, a new method involving SA as fluorescence-enhancing reagent for estimation of BRD in aqueous samples has been suggested. The detection limits of bromadiolone under the optimum conditions were 0.77 and 0.19 µg mL⁻¹ in presence of BSA and HSA, respectively.

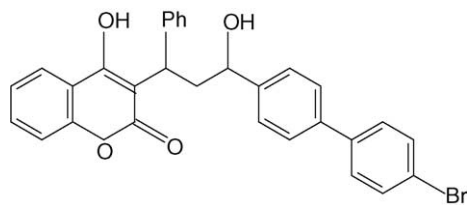
© 2005 Elsevier B.V. All rights reserved.

1. Introduction

Serum albumin (SA), the important protein in the circulatory system, is one of the most extensively studied of all proteins [1–3]. It is synthesized in the liver, exported as a non-glycosylated protein, and is present in the blood at around 40 mg mL⁻¹ [4]. It is the major transport protein for unesterified fatty acids, but is also capable of binding an extraordinarily diverse range of metabolites, drugs and organic compounds. The remarkable binding properties of albumin accounts for the central role, it can play in both the efficacy and rate of delivery of drugs. Many drugs, including anti-coagulants, tranquilizers and general anesthetics, are transported in the blood while bound to albumin [5]. This has stimulated much interest on the nature of the drug binding sites and investigations of whether fatty acids, natural metabolites and drugs compete with one another for binding to the protein [1,2]. These studies provide information on the struc-

tural features that determine the therapeutic effectiveness of drugs. The molecular interactions are often monitored by using optical techniques. These methods are sensitive and relatively easy to use whereas fluorescence spectroscopy is a valuable technique for study of the binding of ligands to proteins. Coumarins constitute an important group of natural products and many of their analogues are found to be biologically active. 4-Methylcoumarin has been found to possess a wide range of biological activities like chloretic, analgesic, anti-spermogenetic, anti-fungal, anti-coagulant and diuretic properties [6]. Interactions of several 7-aminocoumarins with human serum albumin (HSA) and the probable location of these coumarins in domain II have been reported by using fluorescence spectroscopic technique and modeling studies [7]. Coumarin anti-coagulants have been used for a number of years for prophylactic purposes in thromboembolism. Many of these agents are bound to serum proteins, especially SA. This binding affects their pharmacologic and pharmacokinetic properties. Bromadiolone(3-[3-(4'-bromobiphenyl-4-yl)-3-hydroxy-1-phenylpropyl]-4-hydroxycoumarin) (BRD) (Scheme 1) is a coumarin based anti-coagulant rodenticide,

* Corresponding author. Tel.: +91 44 2257 8251; fax: +91 44 2257 8241.
E-mail address: mishra@iitm.ac.in (A.K. Mishra).



Scheme 1. Chemical structure of bromadiolone.

which impairs blood coagulation, leading to hemorrhage as the ultimate cause of death. When compared to warfarin, an effective oral anti-coagulant in humans, it has a high acute toxicity. It shows anti-coagulant effect based on the prothrombin inhibition. Residues of anti-coagulants present in the bodies of dead or dying rodents can be toxic to scavengers, predators and indirectly to man. It has been suggested that HSA serves as a carrier to transport rodenticides to molecular targets and their toxicity effect is directly linked with their HSA binding.

It is important to study the determination and the interaction of BRD and SA due to its high toxicity to all mammals. Several sensitive high performance liquid chromatographic (HPLC) methods have been reported for the determination of BRD in a mixture with other rodenticides in human serum, plasma and animal tissues [8–13]. The association of six rodenticides with HSA and the role of magnesium and calcium on this association have been studied recently by Andre and Guillaume using perturbation method [14]. A theoretical treatment has been developed to describe the association between rodenticides and HSA and the role of sodium cation and saccharose were analysed [15].

In this paper, we studied the binding and the effect of energy transfer between BRD and SA, by spectrofluorimetry. Moreover, the fluorescence method was successfully applied for the determination of BRD.

2. Experimental

2.1. Reagents

BRD was provided by Forensic Science Department, Chennai. Methanol, sodium hydrogen phosphate and disodium hydrogen phosphate were obtained from s.d fine chemicals. Bovine serum albumin (BSA) and HSA Fraction V powder (containing 98–99% of albumin) was obtained from Sigma–Aldrich and used as such. The water used was triple distilled. To adjust the pH of the solution, phosphate buffer (pH 7.0; 0.01 M) was used.

2.2. Apparatus

A Perkin-Elmer lambda 25 UV–vis spectrophotometer was used for the absorbance measurements. pH was measured on an Elico (Model L1 –120) pH meter. Fluorescence

measurements were recorded using Hitachi F-4500 spectrofluorimeter equipped with a 1 cm path length quartz cell. Experiments were performed at two excitation wavelengths, 280 nm (the longest wavelength absorption maximum of Trp) and 330 nm (the longest wavelength absorption maximum for BRD). The slit widths were 5 nm/5 nm, PMT voltage was kept at 700 V and scan speed was 1200 nm s⁻¹.

The fluorescence anisotropy (r_{ss}) values were obtained using the expression $r_{ss} = (I_{||} - GI_{\perp}) / (I_{||} + 2GI_{\perp})$, when $I_{||}$ and I_{\perp} are fluorescence intensities when the emission polarizer is parallel and perpendicular, respectively, to the direction of polarization of the excitation beam, and G is the factor that corrects for unequal transmission by the diffraction gratings of vertically and horizontally polarized light.

2.3. Experimental methods

BRD is sparingly soluble in water. Stock solution of BRD (10^{-3} M) was prepared in absolute ethanol and sonicated for 5 min. Further dilutions were made with triple distilled water in a volumetric flask. SA and BRD solutions were prepared in 0.01 M phosphate buffer (pH 7.00). For quenching experiments, BSA or HSA solutions (3×10^{-6} M) were transferred into 5 mL volumetric flasks and BRD solutions of appropriate concentrations were added in different amounts to the flask. The mixture was diluted to the mark with triple distilled water and mixed thoroughly. The samples were excited at 280 nm and the fluorescence intensity was monitored at 300–500 nm.

3. Results and discussion

3.1. Absorption and fluorescence spectra

The absorption spectra of BRD in SA are given in Fig. 1. The longest wavelength maximum absorption band of BRD is 330 nm. With the addition of SA, the absorption spectra show a slight blueshift with a strong absorbance at 280 nm corresponding to Trp.

Fig. 2 shows the effect of BSA (b) and HSA (c) on BRD emission. In both the cases, a substantial enhancement of BRD fluorescence intensity (F) accompanied by a blueshift of the fluorescence band was observed when excited at 330 nm. Previous studies on interaction of several coumarins with BSA [16] and HSA [7,16] have shown that there is an appreciable enhancement and blueshift of fluorescence when the molecule binds to SA. Similar large enhancement and an appreciable blueshift have been observed for many coumarins in homogeneous solutions with reduction in polarity [17] and also on complexation with cyclodextrins. The hydrophobic interior of SA is less polar than the bulk aqueous phase. Thus, the large enhancement and the blueshift of the fluorescence emission can be attributed to the suppression of k_{nr} (non-radiative processes) and the reduced polarity of the environment. It was also observed that there is an appreciable enhancement of steady state fluorescence anisotropy (r_{ss})

Table 1
Fluorescence spectral characteristics of BRD in water and SA

F_{SA}/F_{water}	λ_{ex} (nm)	λ_{em} (nm)		Anisotropy (r_{ss})		Binding constant (K_A) ($L mol^{-1}$)
		Water	SA	Water	SA	
BSA						
15	330	397.0	386.0	0.12	0.28	7.5×10^4
HSA						
18	330	397.0	386.0	0.12	0.28	3.7×10^5

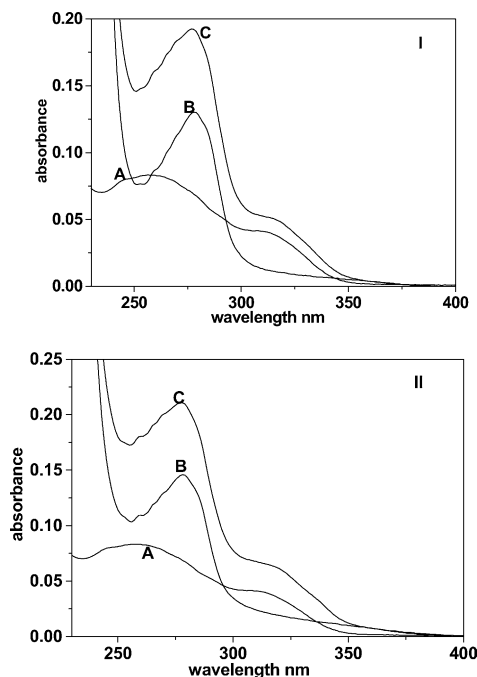


Fig. 1. UV absorption spectra of BSA (I) and HSA (II) in presence of BRD. (I) (A) [BRD] 3×10^{-6} M; (B) [BSA] 3×10^{-6} M; (C) BRD–BSA complex, [BRD] 3×10^{-6} M–[BSA] 3×10^{-6} M. (II) (A) [BRD] 3×10^{-6} M; (B) [HSA] 3×10^{-6} M; (C) BRD–HSA complex, [BRD] 3×10^{-6} M–[HSA] 3×10^{-6} M.

of BRD in BSA and HSA (Table 1). Increase in anisotropy is related to restricted rotational mobility of the fluorescing molecule. Thus, the enhancement of fluorescence intensity, the appreciable fluorescence anisotropy values and the

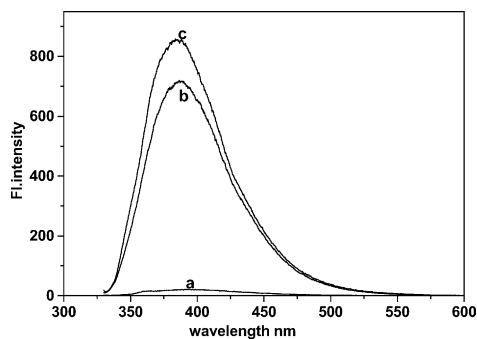


Fig. 2. Fluorescence emission spectra of BRD 3×10^{-6} M in aqueous (a), BSA (b) and HSA (c) media. [BRD] = 3×10^{-6} M; [BSA] = 9×10^{-6} M; λ_{ex} = 330 nm.

blueshift of emission in presence of SA indicate partitioning of BRD to a restrictive and hydrophobic binding site in SA. This behavior of BRD is in line with the fluorescence behavior of various other coumarins in BSA [16] and HSA [7] suspensions. The data are summarized in Table 1.

3.2. Binding constant of serum albumin with BRD

3.2.1. Quenching experiments

HSA and BSA consist of amino acids chains forming a single polypeptide with well-known sequence, which contain three homologous α -helices domains (I–III). Each domain contains 10 helices and is divided into anti-parallel six-helix and four sub-domains (A and B). The adherence of two sub-domains, with their grooves towards each other forms a domain, and three of such domains make up an albumin molecule [18,19]. HSA binds reversibly to a large number of endogenous and exogenous compounds. The capacity of binding aromatic and heterocyclic compounds depends largely on the existence of two major binding regions, namely Sudlow's site I (or benzodiazepine site) and Site II (or warfarin site), which are located within specialized cavities in sub-domains IIA and IIIA, respectively [14].

HSA and BSA solutions when excited at 290 nm emit fluorescence attributable mainly to tryptophan residues [20]. HSA contains 585 amino acid residues with only one tryptophan located at position 214 along the chain, in sub-domain IIA. BSA molecule is formed by 582 amino acid residues, and contains a first tryptophan residue in position 134, in sub-domain IB of the albumin molecule, and a second tryptophan residue in position 212, in sub-domain IIA [18].

As Fig. 1 shows, excitation at 330 nm preferentially excites BRD, whereas excitation at 280 nm preferentially excites Trp. Fig. 3 shows the fluorescence spectra under 280 nm excitation in solutions containing a fixed concentration (3×10^{-6} M) of SA and varying concentration of BRD in the range 0 – 8×10^{-7} M. Under these conditions, direct excitation of BRD is avoided. With progressive addition of BRD solution to SA suspension, the Trp emission at 335 nm decreases with a concomitant increase in the BRD emission. This effect is highly pronounced for HSA in which a clear BRD emission band is seen with maximum at 385 nm. Clearly, a Förster type fluorescence resonance energy transfer (FRET) mechanism is involved in this quenching of Trp fluorescence by BRD in BRD–SA complexes. An isoemissive point at 350 nm is seen, indicating that the quenching of protein fluorescence

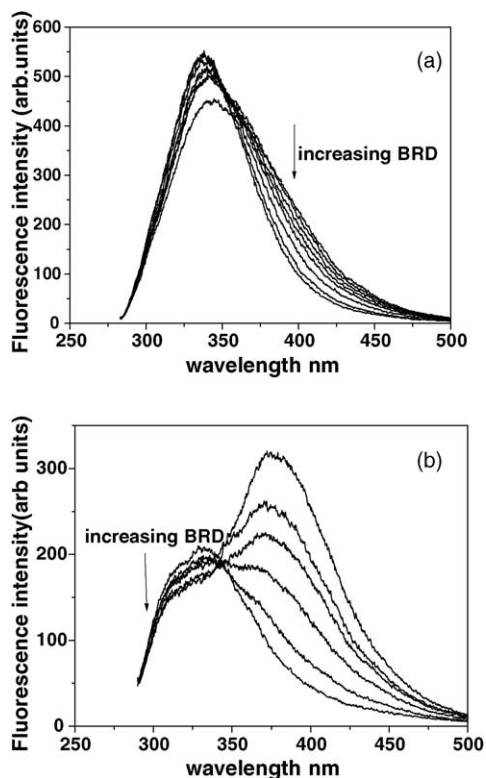


Fig. 3. Fluorescence spectra of BSA (a) and HSA (b) at various concentration of BRD. [BSA] = [HSA] = 3×10^{-6} M; [BRD] $0-8 \times 10^{-7}$ M; $\lambda_{\text{ex}} = 280$ nm.

depends on the formation of bound BRD with BSA or HSA. It can be noted that the maximum of 385 nm observed for BRD–HSA complex when excited at 280 nm is a little further blueshifted compared to the corresponding maximum of 394 nm when excited at 330 nm. This clearly shows that the BRD emission observed at 280 nm excitation originates from only the completely SA-bound BRD.

The Stern–Volmer and Lineweaver–Burk graphs are shown in Fig. 4 for the interaction of BRD in presence of HSA and BSA. Fig. 4(a) shows that the curves have fine linear relationships according to the quenching equation:

$$\frac{F_0}{F} = 1 + k_q \tau_0 [Q] = 1 + K_{SV} [Q], \quad (1)$$

where k_q , K_{SV} , τ_0 and $[Q]$ are the quenching rate constants of the biomolecule, the dynamic quenching constant and the average lifetime of the molecule without the quencher, respectively. $K_{SV} = k_q \tau_0$, $k_q = K_{SV} / \tau_0$. Taking fluorescence lifetime of Trp in SA at around 10^{-8} s [21], an approximate quenching constant (k_q , $\text{L mol}^{-1} \text{s}^{-1}$) can be obtained by the slope: $k_q = 1.2 \times 10^{13} \text{ M}^{-1} \text{ s}^{-1}$ ($r = 0.991$) for BSA and $2.5 \times 10^{13} \text{ M}^{-1} \text{ s}^{-1}$ ($r = 0.983$) for HSA. However, the maximum dynamic collisional quenching constant of various kinds of quenchers for biopolymers fluorescence is around $2.0 \times 10^{10} \text{ L mol}^{-1} \text{ s}^{-1}$ [22]. Thus, the rate constant of protein quenching procedure initiated by BRD is greater than k_q of scatter procedure. This indicates that a static quenching mechanism is operative. The Lineweaver–Burk equation for

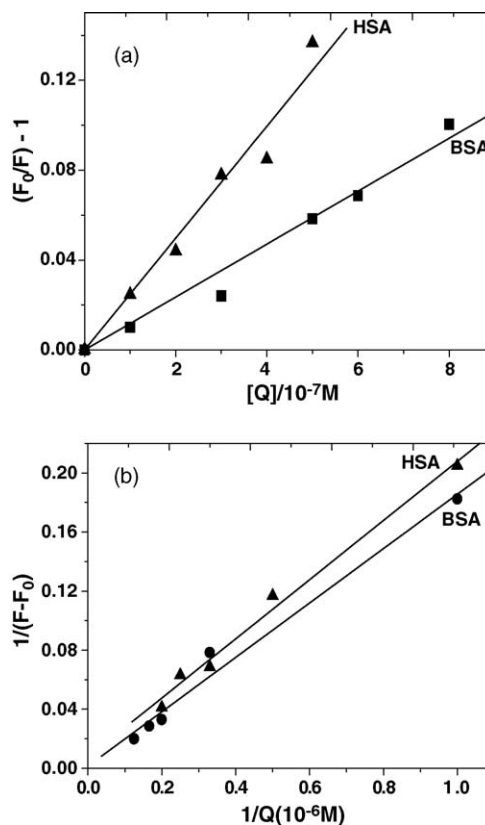


Fig. 4. Stern–Volmer curves (a) and Lineweaver–Burk curves (b). [BSA] = [HSA] = 3×10^{-6} M; $\lambda_{\text{ex}} = 280$ nm.

static quenching is [23]

$$\frac{1}{F_0 - F} = \frac{1}{F_0} + \frac{K_D}{F_0 [Q]} \quad (2)$$

Using this, the formation constant (K_A , L mol^{-1}) can be obtained from Fig. 4(b). ($K_A = 1/K_D$): BSA, $K_A = 7.5 \times 10^4$, $r = 0.99$; HSA, $K_A = 3.7 \times 10^5$, $r = 0.9$.

It shows a reasonably strong binding constant between BRD and serum albumin. The higher binding constant of BRD with HSA as compared to BSA is expected. As was seen in Fig. 2, for the same concentration of BRD, BSA and HSA, the fluorescence intensity of the BRD–HSA system was higher.

The fluorescence quencher interacts in the hydrophobic protein sub-domain containing Trp residues. The main HSA binding regions are located in sub-domains IIA and IIIA as it results from the crystallography study of X-ray diffraction for several ligands [24]. Anti-coagulant rodenticides can bind either on the low affinity site (site I, benzodiazepine site) or the high affinity site (site II, warfarin site). Alkyl-coumarins, drugs containing coumarin moiety, like warfarin and several coumarin anti-coagulants, are known to bind to domain II and site I of HSA [25–29]. Andre and Guillaume [14,15] calculated various thermodynamic parameters for the two HSA sites in presence of six anti-coagulant rodenticides. It was shown that, among the coumarin family,

BRD association with HSA was greatest because of steric hindrance. It exhibited the lowest thermodynamic data for the site II. This has been explained due to its high hydrophobicity and the Br substituent which was responsible for an additional solute polar interaction with HSA. Binding of many coumarins to domain IIA of HSA is known to result in significant enhancement of coumarin fluorescence [7]. The enhancement of BRD fluorescence appears to follow the same pattern. In BSA, the tryptophan residues could be either Trp 135 or Trp 214. Of both tryptophans in BSA, Trp 135 is more exposed to a hydrophilic environment, whereas Trp 214 is deeply buried in the hydrophobic loop. Comparing the quenching effect of the same quencher on the HSA (Trp 214) and BSA (Trp 135 and Trp 214) spectra, the quenching efficiency is very similar for the two proteins, thereby suggesting that Trp 214 is involved in the quenching process in SA.

3.3. Energy transfer between BRD and SA

The overlap of UV absorption spectra of BRD with the fluorescence emission spectra of BSA (a) or HSA (b) is shown in Fig. 6. According to Förster's non-radiative energy transfer [30], the rate of energy transfer depends on: (i) the relative orientation of the donor and acceptor dipoles, (ii) the extent of overlap of the emission spectrum of the donor with the absorption spectrum of the acceptor and (iii) the distance between the donor and the acceptor. The energy transfer effect is related not only to the distance between the acceptor and the donor, but also on the critical energy transfer distance R_0 , that is:

$$E = \frac{R_0^6}{R_0^6 + r^6} \quad (3)$$

where r is the distance between the acceptor and the donor and R_0 is the critical distance when the transfer efficiency is 50%, which can be calculated by

$$R_0^6 = 8.8 \times 10^{-25} K^2 \phi J n^{-4} \quad (4)$$

where K^2 is the spatial orientation factor between the emission dipole of the donor and the absorption dipole of the acceptor. The dipole orientation factor, K^2 , is the least certain parameter in calculation of the critical transfer distance, R_0 . Although theoretically K^2 can range from 0 to 4, the extreme values require very rigid orientations. If both the donor and acceptor are tumbling rapidly and free to assume any orientation, then K^2 equals 2/3 [31]. If only the donor is free to rotate, then K^2 can vary from 1/3 to 4/3 [32,33], n is the refractive index of the medium, ϕ the fluorescence quantum yield of the donor and J is the overlap integral of the fluorescence emission spectrum of the donor and the absorption spectrum of the acceptor, given by

$$J = \frac{\sum F(\lambda)\varepsilon(\lambda)\lambda^4 \Delta\lambda}{\sum F(\lambda)\Delta\lambda} \quad (5)$$

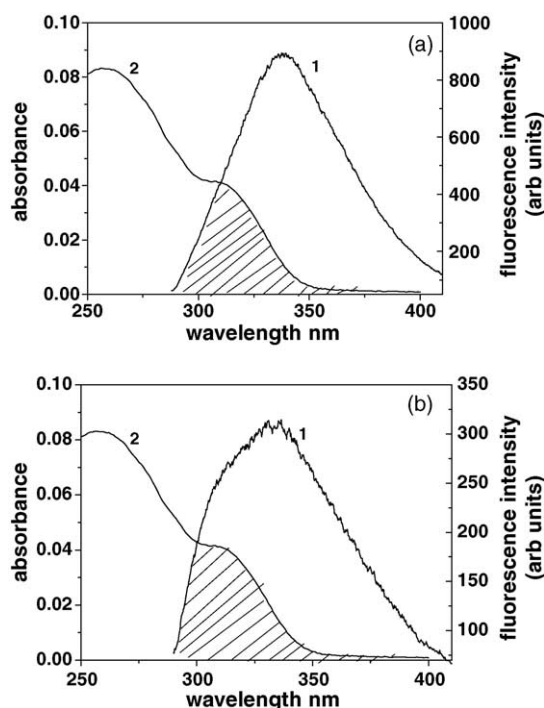


Fig. 5. (a) Overlap of the fluorescence spectra of BSA (1) with the absorption spectra (2) of BRD. (b) Overlap of the fluorescence spectra of HSA (1) with the absorption spectra (2) of BRD.

where $F(\lambda)$ is the fluorescence intensity of the fluorescent donor in wavelength λ and is dimensionless, $\varepsilon(\lambda)$ the molar absorption coefficient of the acceptor in wavelength λ and its unit is $\text{cm}^{-1} \text{mol}^{-1} \text{L}$. The energy transfer efficiency is frequency calculated from the relative fluorescence yield in the presence (F) and absence of acceptor (F_0):

$$E = \frac{1 - F}{F_0} \quad (6)$$

J can be evaluated by integrating the spectra in Fig. 5. It has been reported for BSA, that $K^2 = 2/3$, $\phi = 0.15$ and $n = 1.36$ [34]. Based on these data, we found $R_0 = 5.6$ nm and $r = 2.6$ nm for BSA, and $R_0 = 6.6$ nm and $r = 4.5$ nm for HSA. So the distance between BRD and Trp residue in BSA or HSA is about 2.6 and 4.5 nm, respectively. These values are rather approximate. However, the distances obtained this way agree well with literature values of substrate binding to SA at site IIA [35,36]. The larger R_0 value obtained for HSA is indicative of more efficient FRET observed in the BRD–HSA complex.

3.4. Determination of BRD

There is a significant enhancement of fluorescence intensity in presence of SA, which could be used in developing an analytical method for determination of BRD.

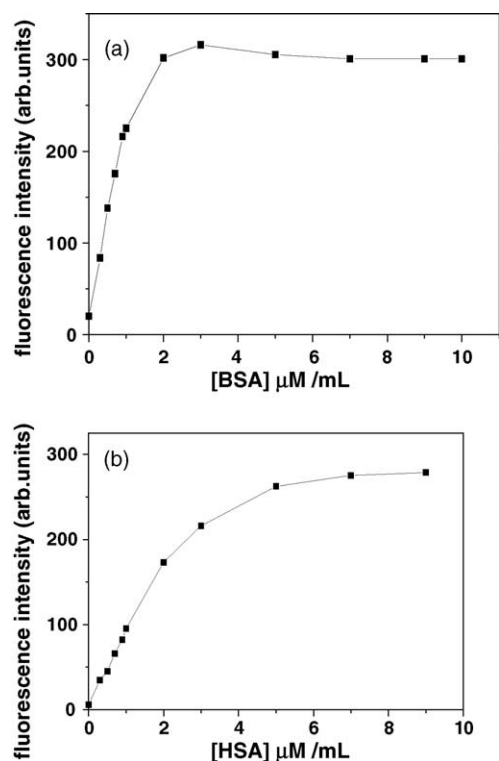


Fig. 6. Variation of fluorescence intensity on BRD (3×10^{-6} M) in presence of (a) BSA, (b) HSA. [BSA]=[HSA]= $0-1 \times 10^{-5}$ M; $\lambda_{\text{ex}}=330$ nm; $\lambda_{\text{em}}=390$ nm.

3.4.1. Optimization of experimental conditions for the determination of BRD

In order to select an optimized analytical system experimental parameters like pH, concentration of SA were studied at [BRD] 3×10^{-6} M.

The influence of pH was studied in the range of 3–10 using phosphate buffer. The stable fluorescence intensity for the BRD–SA complex was achieved at pH 6–8. Hence, phosphate buffer (0.01 M) at pH 7.0 was used in this work.

For the spectrofluorimetric determination of BRD in SA, the BSA or HSA concentration was varied from 3×10^{-7} to 1×10^{-5} M by fixing the BRD concentration at 3×10^{-6} M. As expected, there was a substantial enhancement of fluorescence intensity in presence of SA, which remained constant after a particular concentration [3×10^{-6} M] (Fig. 6). Therefore, fixing the SA concentration at 3×10^{-6} M, the emission spectra were recorded at excitation 330 nm, for various concentration of BRD [1×10^{-7} to 3×10^{-6} M] in order to determine the analytical parameters (Fig. 7).

3.5. Method of validation

The parameters determined in this study were linearity, detection and quantitation limits, precision, selectivity and robustness. Tables 2 and 3 summarize the results obtained from statistical analysis of the data.

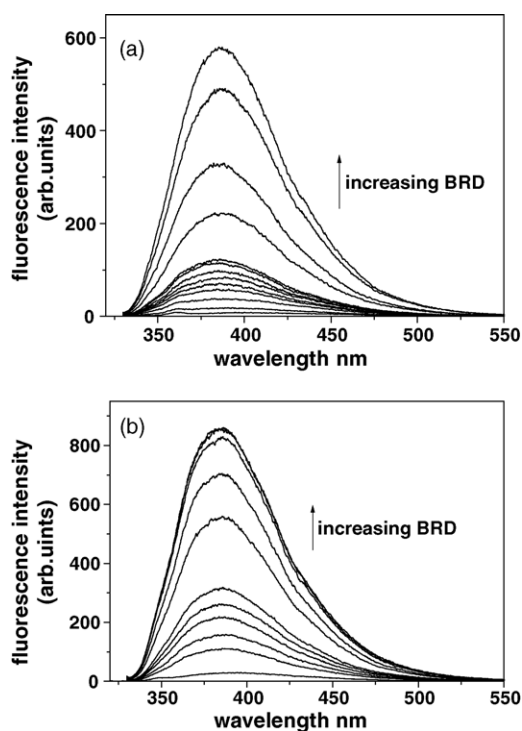


Fig. 7. Fluorescence emission spectra of BSA (a) and HSA (b) in presence of varying concentration of BRD. [BRD] 1×10^{-7} M to 3×10^{-6} M; $\lambda_{\text{ex}}=330$ nm.

3.5.1. Linearity

The equation for calibration graph in all cases is $F=h+mC$, where F is the fluorescence intensity (in arbitrary units) and C is the concentration of BRD expressed in $\mu\text{g mL}^{-1}$. The calibration graph of fluorescence intensity (F) versus the BRD concentration (C) was drawn and found to be linear in the range 1.5–31.6 and 0.5–36.9 $\mu\text{g mL}^{-1}$ in presence of BSA and HSA, respectively [36–38]. For the goodness of the calibration curve, the coefficient of determination (R^2) was found to be 0.99 in both the cases and the regression was found to be significant by performing the ‘ F -test’ (Table 2).

Table 2
Analytical parameters of BRD determination in presence of BSA or HSA

	BSA	HSA
Linear dynamic range ($\mu\text{g mL}^{-1}$) (LDR)	1.5–31.6	0.5–36.9
Intercept on the ordinate (a)	18.89	13.81
S.D. of the intercept on the ordinate (S_a)	4.9	1.2
Slope (b)	19.09	18.66
S.D. of slope (S_b)	3.15	5.51
No. of points	11	11
Coefficient of correlation (r)	0.99	0.99
Detection limit ($\mu\text{g mL}^{-1}$)	0.77	0.19
Quantification limit ($\mu\text{g mL}^{-1}$)	2.57	0.64
Analytical sensitivity (S_A)	0.073	0.085
Coefficient of determination (R^2)	0.99	0.99

Table 3
Results for robustness study

Conditions					
Concentration of SA	1.5×10^{-6} M, pH 6.00	1.5×10^{-6} M, pH 8.00	2.4×10^{-6} M, pH 6.00	2.4×10^{-6} M, pH 8.00	Mean
Results					
For BSA, R.S.D. (%)	3.15	3.6	3.0	2.0	2.93
For HSA, R.S.D. (%)	3.0	3.5	2.5	2.0	2.75

3.5.2. Detection and quantitation limits

The detection and quantification limits were calculated as $3s_b/m$ and $10s_b/m$, where s_b is the standard deviation of the intercept and m is the slope of the calibration graph (Table 2).

3.5.3. Precision, selectivity and sensitivity

The relative standard deviation are 3.3% (BSA) and 3.0% (HSA), as obtained from 11 replicate determinations of 3×10^{-6} M of SA solutions at pH 7. The selectivity of the method was checked by adding metal ion interferants like Na^+ , K^+ and Mg^{2+} and experimental results showed that the fluorescence intensity of BRD in SA was hardly affected by them. The gradient of the calibration graph is the sensitivity of a method according to the IUPAC definition [39]. The sensitivity of the method is reported as the analytical sensitivity, $S_A = s_s/m$ (s_s is the standard deviation of the analytical signal) (11 measurements) and m is the slope of the calibration graph. (Table 2).

3.5.4. Robustness

The consistency of an analytical method, robustness is defined by its capacity to produce constant and unbiased results when it is applied under different operating conditions [40]. When the intrinsic operating conditions of a method are slightly modified, robustness can be determined.

To demonstrate the robustness of the method, the sample solutions were prepared in duplicate under different conditions of sample treatment. Experimental parameters such as concentration of SA and pH were varied to evaluate the robustness of the method. Thus, concentration of SA was varied at 50% (1.5×10^{-6} M) and 80% (2.4×10^{-6} M) and pH 6.00 and 8.00 from the nominal values of 3×10^{-6} M and pH 7.00. The R.S.D.% was calculated under these conditions. These results as shown in Table 3 are fairly independent on the working conditions, since small variations in the main variables of the method do not affect significantly the results.

4. Conclusion

There is a reasonably strong binding of BRD to SA which results in a significant enhancement of BRD fluorescence. Based on this, a new method involving SA as fluorescence-enhancing reagent for estimation of BRD in aqueous samples is suggested here. The analytical parameters obtained for this appeared to be fairly good. Although in this work an excitation wavelength of 330 nm has been chosen which prefer-

entially excites BRD, it may be noted that if HSA is used as reagent the excitation wavelength range available can be extended to around 280 nm. This is because of a more efficient FRET observed in BRD–HSA complex.

Acknowledgements

We thank Mrs. Kala, Forensic Science Department, Chennai, for providing BRD sample. S.D. thanks Council of Scientific and Industrial Research, CSIR New Delhi for fellowship.

References

- [1] T. Peters, Biochemistry, Genetics and Medical Applications, Academic Press, San Diego, CA, 1996.
- [2] K. Hansen, Dan. Med. Bull. 37 (1990) 57–84.
- [3] D.C. Carter, J.X. Ho, Adv. Protein Chem. 45 (1994) 153–203.
- [4] S. Curry, H. Mandelkow, P. Brick, N. Franks, Nat. Struct. Biol. 5 (1998) 827–835.
- [5] H.P. Rang, M.M. Dale, J. Ritter, Mol. Pharmacol., third ed., Churchill Livingstone, New York, 1995.
- [6] K. Chinnakali, H.-K. Fun, K. Sriraghavan, V.T. Ramakrishnan, Acta Crystallogr. C54 (1998) 542–544.
- [7] J. Shobini, A.K. Mishra, K. Sandhya, N. Chandra, Spectrochim. Acta 57 (2001) 1133–1147.
- [8] F. Guan, A. Ishii, H. Seno, K. Watanabe, T. Kumazawa, O. Suzuki, J. Pharm. Biomed. Anal. 21 (1) (1999) 179–185.
- [9] V. Fauconnet, H. Pouliquen, L. Pinault, J. Anal. Toxicol. 21 (7) (1997) 548–553.
- [10] M.F. Morrin, N. Merlet, M. Dore, J.C. Lechevin, Analusis 17 (9) (1989) 526–531.
- [11] K. Hunter, E.A. Sharp, A. Newton, J. Chromatogr. 435 (1988) 83–95.
- [12] K. Hunter, J. Chromatogr. 321 (1985) 255–272.
- [13] S. Panadero, A. Gomez-Hens, D. Perez-Bendito, Talanta 40 (1993) 225–230.
- [14] C. Andre, Y.C. Guillaume, J. Chromatogr. B 801 (2004) 221–227.
- [15] C. Andre, Y.C. Guillaume, Chromatographia 59 (2004) 429–436.
- [16] A. Nag, K. Bhattacharya, Chem. Phys. Lett. 169 (1990) 12–16.
- [17] G. Jones, W.P. Jackson, C.Y. Choi, J. Phys. Chem. 89 (1985) 294–300.
- [18] K.H. Ulrich, Pharm. Rev. 33 (1981) 17–54.
- [19] I. Peptitas, T. Gruine, A.A. Bhattacharya, S. Curry, J. Mol. Biol. 314 (2001) 955–960.
- [20] J.R. Lakowicz, Principles of Fluorescence Spectroscopy, second ed., Kluwer Academic Publishers/Plenum Press, New York, 1999.
- [21] J.R. Lakowicz, G. Weber, Biochemistry 12 (1973) 4161–4170.
- [22] W.R. Ware, J. Phys. Chem. 66 (1962) 455–458.
- [23] G.Z. Chen, X.Z. Huang, J.G. Xu, Z.Z. Wang, Z.Z. Zheng, The Methods of Fluorescence Analysis, second ed., Science Press, Beijing, 1990, 2–39.
- [24] X. Min he, D. Carter, Nature 358 (1992) 209–215.

- [25] M. Irikura, A. Takadate, S. Goya, M. Otagiri, *Chem. Pharm. Bull.* 39 (1991) 724–728.
- [26] D.J. Birkett, S.P. Meyer, G. Sudlow, *Mol. Pharmacol.* 13 (1977) 987–992.
- [27] I. Sjöholm, Binding of drugs to human serum albumin, in: *Proceedings of the 11th FEBS Meeting*, vol. 50, Copenhagen, 1977, pp. 71–78.
- [28] K.J. Fehske, W.E. Muller, U. Wollert, *Biochim. Biophys. Acta* 577 (1979) 346–359.
- [29] W.E. Muller, U. Wollert, *Pharmacology* 19 (1979) 59–67.
- [30] T. Forster, in: O. Sinanoglu (Ed.), *Modern Quantum Chemistry*, 3, Academic Press, New York, 1996.
- [31] T. Forster, *Discuss. Faraday Soc.* 27 (1959) 7–17.
- [32] C.W. Wu, L. Stryer, *Proc. Natl. Acad. Sci. U.S.A.* 69 (1972) 1104–1108.
- [33] J.R. Lakowicz, *Principles of Fluorescence Spectroscopy*, Plenum Press, New York, 1983 [Chapter 10].
- [34] L. Cyril, J.K. Earl, W.M. Sperry, *Biochemists' Handbook*, E. & F.N. Spon, London, 1961, p. 84.
- [35] J. Liu, J.N. Tian, J. Zhang, Z. Hu, X. Chen, *Anal. Bioanal. Chem.* 376 (2003) 864–867.
- [36] Analytical Methods Committee, *Analyst* 112 (1987) 199–204.
- [37] Analytical Methods Committee, *Analyst* 119 (1994) 2363–2367.
- [38] Analytical Methods Committee, *Analyst* 113 (1988) 1469–1471.
- [39] M. Thompson, S.L.R. Ellison, R. Wood, *Pure Appl. Chem.* 74 (2002) 835–855.
- [40] J.M. Bosque-Sendra, M. Nechar, L. Cuadros-Rodríguez, *Fresenius J. Anal. Chem.* 365 (1999) 480–488.